DETECTION OF STRAIN INDUCED MICROSTRUCTURAL CHANGES IN ALUMINUM (6061-T6) USING ULTRASONIC SIGNAL ANALYSIS*

G.H. Thomas and S.H. Goods

Acceptance Technology Division & Materials Science Div.
Sandia National Laboratories
Livermore, CA 94550

A.F. Emery

Department of Mechanical Engineering
University of Washington
Seattle, WA

ABSTRACT

A correlation between the change in ultrasonic wave forms and applied strain in aluminum (6061-T6) has been obtained at high strain levels. Sophisticated signal processing techniques have indicated a complex interaction of the frequency components of a high frequency ultrasonic pulse as it passes through an aluminum tensile specimen. Strain induced microstructural changes in the aluminum attenuate the acoustic energy. One of the attenuation mechanisms is the formation of deformation induced cavities at precipitates and inclusions which scatter the ultrasonic energy. Measuring the signal attenuation at the appropriate frequencies determines the degree of deformation induced damage.

INTRODUCTION

The ductile fracture of metals and alloys generally occurs by the formation, growth and coalescence of voids or cavities. While the mechanism by which voids or cavities grow may vary with test or

*Work supported by the U.S. Department of Energy under Contract DE-AC04-76DP00789.

exposure temperature, nucleation invariably occurs as the result of plastic deformation.[1-3] Further, the most likely sites for cavity nucleation are in regions where the deformation is inhomogeneous. Thus, in single crystals or within the grains of polycrystals, the nucleation of voids is generally associated with inclusions or rigid second phase particles.[4-7]

A large body of evidence suggests that it is the nucleation of cavities rather than their growth which controls the fracture of materials over a wide range of temperatures.[8,9] This is especially true for materials subject to creep deformation, but may also be important at lower temperatures where time dependent plasticity is generally not a concern. Thus the presence of voids within a material might be a source of ductility loss or mechanical failure in a structural component subject to either continuous or cyclic loading during its service life.

For this reason, it is useful to develop a technique which will indicate the presence of voids within a fabricated part prior to its use. In the past voids have been directly observed via optical or scanning electron microscopy using conventional metallographic techniques. These, of course, are destructive procedures as they require the physical sectioning of the workpiece. Such direct observation is generally difficult due to the small size of void nuclei. Alternatively, density change measurements have been used to measure the increase in void volume fraction. However, given the high sensitivities required, these techniques are often unreliable.

Ultrasonic attenuation measurements provide another opportunity to develop a nondestructive technique for measuring the onset of cavitation either during or subsequent to mechanical deformation. Several researchers [10-15] have noted a sensitivity of ultrasonic attenuation to various material properties and microstructures. Their work has related ultrasonic signal loss with such material properties as fracture toughness,[10] precipitate strengthening,[11] grain size,[12] and other microstructural inhomogeneities.[13-15] This study seeks to correlate ultrasonic attenuation with void nucleation and growth in an aluminum alloy (6061-T6). A technique has evolved to measure energy loss in an ultrasonic pulse as it passes through the tensile specimen. This technique partitions the pulses into several frequency intervals and calculates the energy content of each interval. This nondestructive technique interrogates the bulk material and makes very sensitive measurements of ultrasonic attenuation.

EXPERIMENTAL PROCEDURE

The ultrasonic detection of void nucleation in 6061-T6 aluminum relied on accurate measurements of signal energy at selected frequency intervals. The protocol established to make these measurements is schematically illustrated in Fig. 1 and described in the following text.

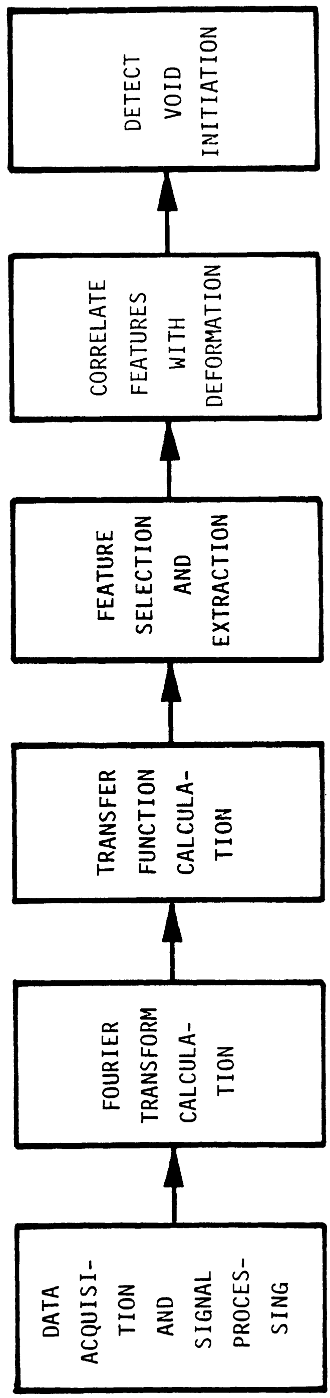

Figure 1. Protocol for ultrasonic detection of void nucleation.

The first block in Fig. 1, data acquisition, involved interrogating the aluminum sample with high frequency (25 MHz), broadband pulses. An Instron mechanical testing machine was fixtured so that the sample and transducer were immersed in water. The rectangular cross-sectioned tensile specimen reflected the acoustic energy from the front surface as well as the back wall. The front surface reflection was considered a reference signal, and the subsequent back surface echoes provided the attenuation information. Figure 2 is a computer plot of a typical R-F waveform. The first pulse was from the water to aluminum interface (front surface reflection), and the remaining pulses were from the back surface of the aluminum. A block diagram of the data acquisition system is shown in Fig. 3. This system consisted of a focused 25 MHz broadband transducer, a Panametrics 5052 PRX pulser/receiver, a Biomation 8100 analog to digital converter, and a PDP 11/34 minicomputer.

The next phase in this procedure (second block in Fig. 1) was to reduce the data. The data reduction was accomplished using a Fast Fourier Transform algorithm[16] to calculate the frequency spectra for each of the pulses. Then, to minimize transducer dependence and acoustic coupling effects, a transfer function was calculated by dividing the complex frequency spectrum of each back surface echo by the complex spectrum front surface echo.[17] The step is indicated in the third block in Fig. 1.

After reducing the data, features of the ultrasonic wave forms pertinent to the detection of void nucleation were selected and extracted. This process involved considerable data manipulation to sort through a large array of features and determine which were useful and which were not. Two categories of features correlated well with plastic deformation in the sample. The first category encompassed amplitude-time domain features. These are indicated in Table 1 as Features 1-6 and were the ratios of the peak to peak amplitudes of each back surface reflection to the front surface reflection. The second kind of feature was frequency related and was extracted from the transfer function domain. These features are listed in Table 1 as Features 7-36 and were the areas under the transfer function curve for selected frequency intervals. They are separated into groups of six, where each of the six features correspond to a different, multiple back surface reflection. An example of a typical transfer function and the way features were extracted is illustrated in Fig. 4. The area under the curve within the dotted lines represents the energy content of the ultrasonic pulse for that frequency interval and was monitored to detect signal attenuation.

The fifth step as shown in Fig. 1 was to note changes in the features as the tensile specimen was deformed. As an example, the plot shown in Fig. 5 compares the area under the transfer function curve in 15-20 MHz range with strain in the aluminum specimen.

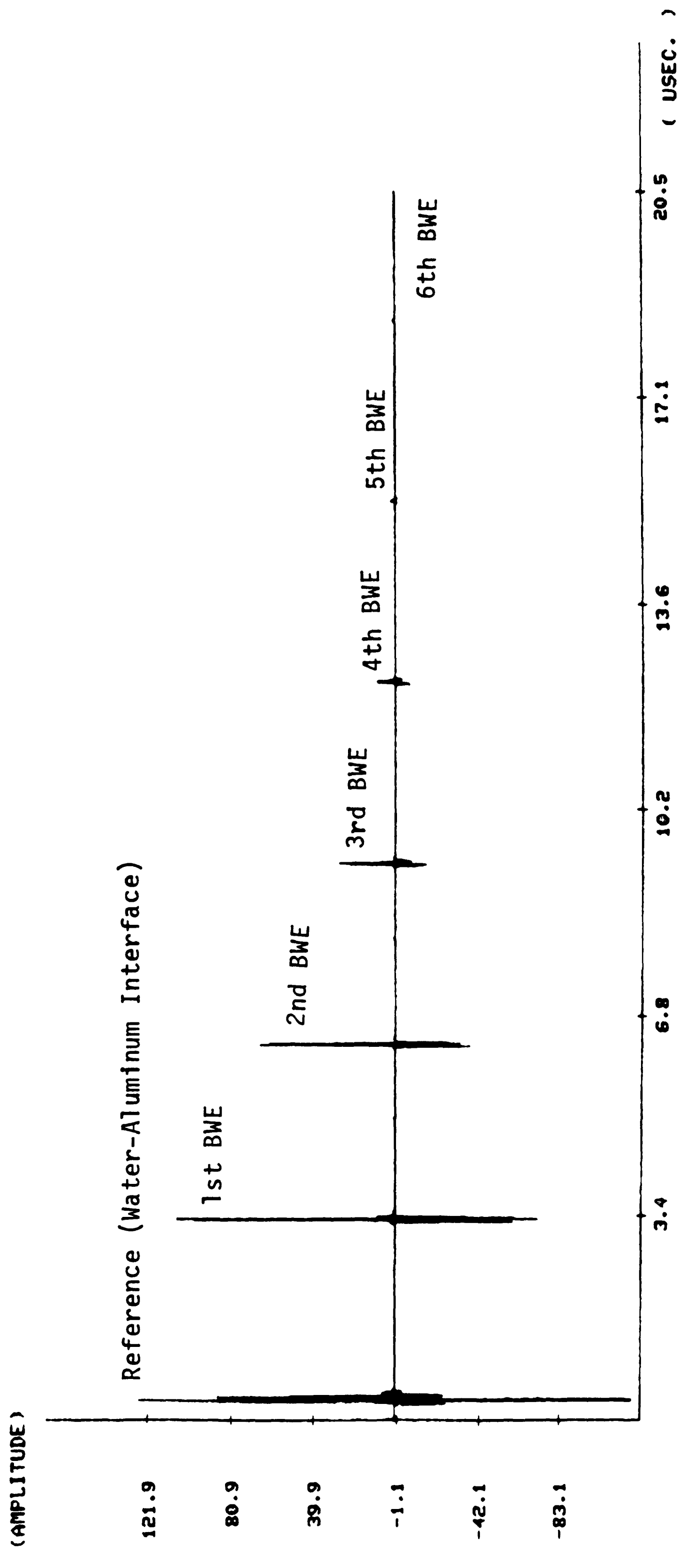

Figure 2. Typical ultrasonic response from the aluminum tensile specimen.

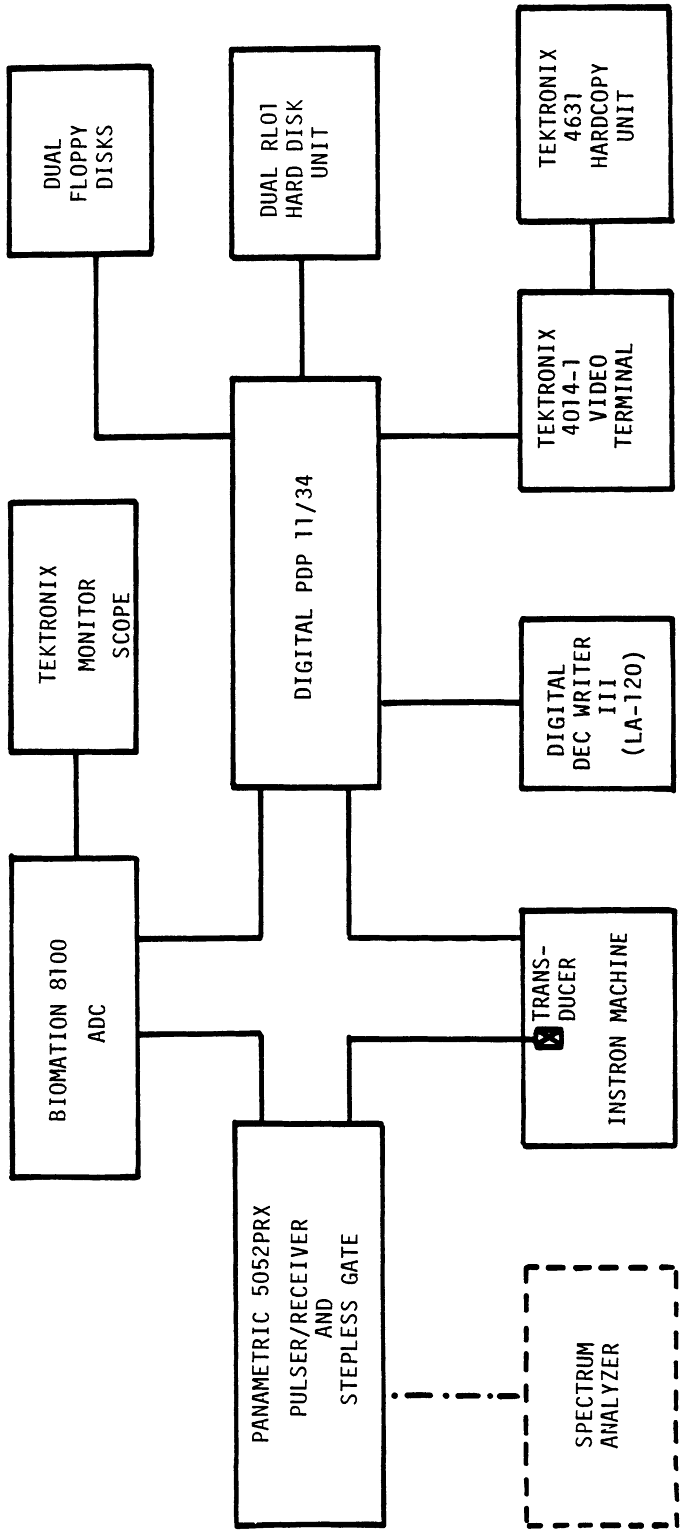

Figure 3. Block diagram of the computerized ultrasonic data acquisition and signal processing system.

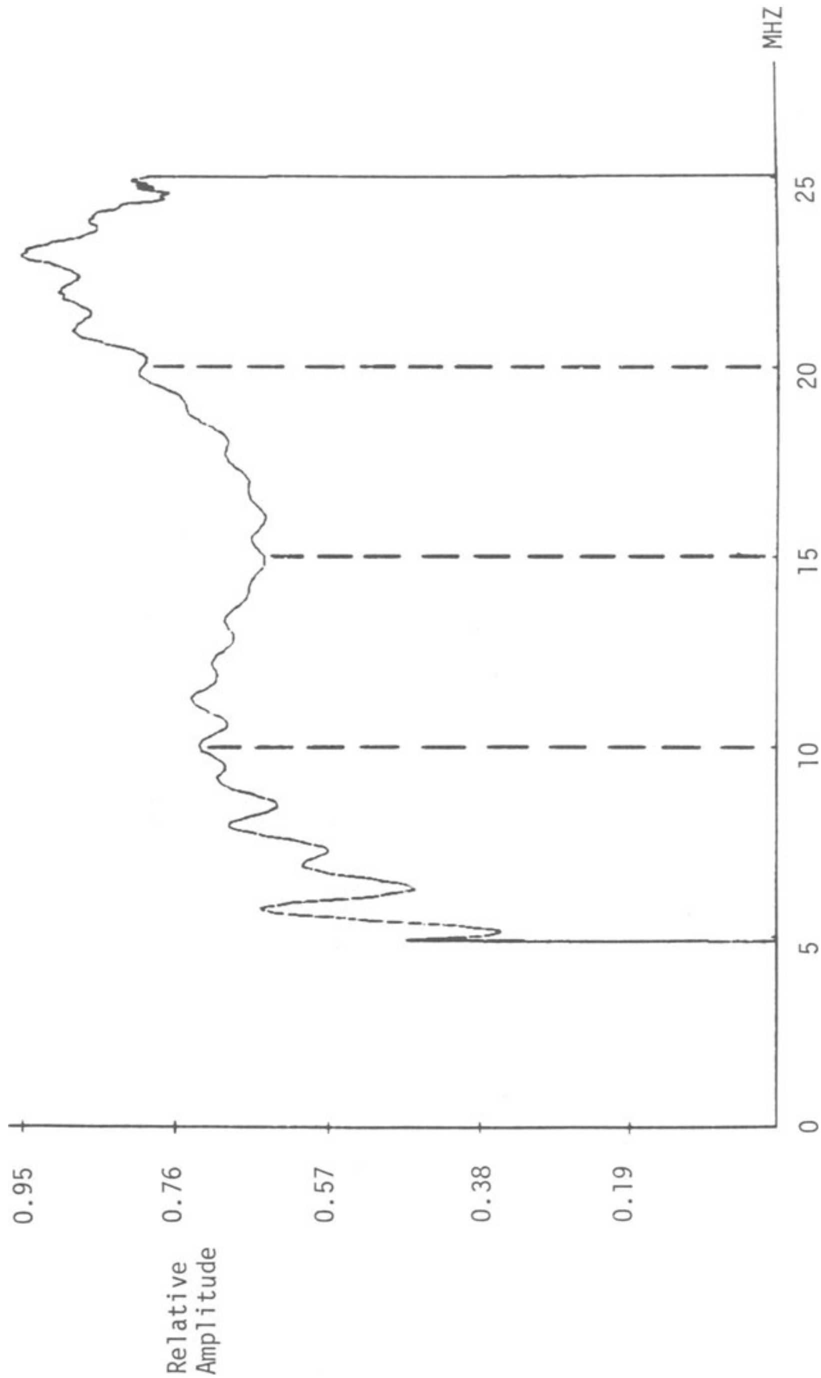

Figure 4. Typical transfer function with frequency intervals indicated.

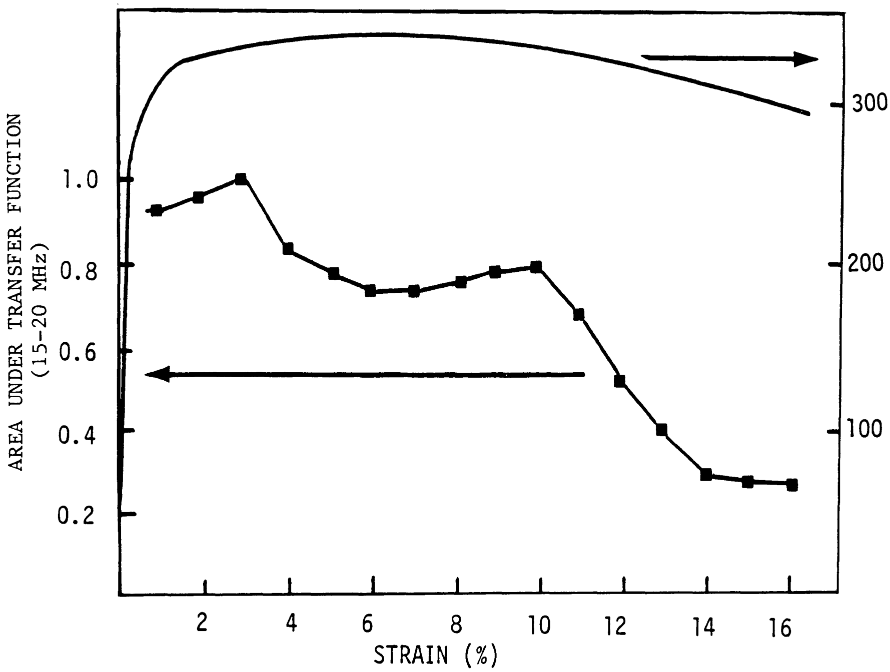

Fig. 5. Area under transfer function (15-20 MHz) vs. engineering strain. Data were acquired as the aluminum tensile sample was loaded.

Table 1. Features Used to Detect Void Nucleation in Aluminum (6061-T6)

Features	
1-6:	Peak to Peak Echo (1-6)/Peak to Peak Reference
7-12:	Area under Transfer Function between 5 and 10 MHz for Echoes 1-6
13-18:	Area under Transfer Function between 10 and 15 MHz for Echoes 1-6
19-24:	Area under Transfer Function between 15 and 20 MHz for Echoes 1-6
25-30:	Area under Transfer Function between 20 and 25 MHz for Echoes 1-6
31-36:	Area under Transfer Function between 5 and 25 MHz for Echoes 1-6

Plotting each of the features listed in Table 1 as a function of strain was a method of determining which features were appropriate in the detection of void nucleation. Understanding the correlation between ultrasonic attenuation and void formation will allow us to develop a procedure to detect the onset of void nucleation. This goal is shown as the last block in Fig. 1.

Two complementary data acquisition procedures were developed. First, ultrasonic data were acquired in situ at fixed strain intervals during tensile testing. Part-way through the test the specimen was removed and the reflecting surfaces were machined flat and parallel. The specimen was then remounted in the tensile fixture and the test continued. In this way, deformation induced texture and necking induced surface curvature were eliminated as possible sources of attenuation. The second procedure was to deform the specimen to a strain near fracture and remove it from the mechanical testing machine. The reflecting surfaces of the deformed specimen were then milled flat and parallel, which again eliminated surface texture and curvature as possible sources of attenuation. After machining, the sample was placed in a computer controlled X-Y scanner and the necked region was scanned parallel to the tensile axis. This scanning process allowed ultrasonic data to be taken at uniform intervals along the gage length of the samples. Measuring the reduction of cross sectional area at these same intervals on the specimen provided a way to compare ultrasonic signal attenuation with the local strain.

RESULTS AND DISCUSSION

A relationship between ultrasonic signal attenuation and deformation induced void formation in the test alloy (aluminum 6061-T6) has been established. Results from the method where data were acquired during the sample deformation are shown in Fig. 5. This figure is a plot of the area under the transfer function curve between 15-20 MHz for the second back wall reflection (Feature 20 in Table 1) as a function of engineering strain. This curve indicates an abrupt decrease in signal strength for this feature at approximately ten percent strain. Since cavities within the specimen will act as scattering sites, and since curvature and surface texture were eliminated as possible sources of the attenuation, this decrease in signal strength may be an indication of void formation in the alloy. The results of the second data acquisition method are shown in Fig. 6. Figure 6a is a graph of the area under the transfer function in the 15-10 MHz range for the second back wall reflection (Feature 20) versus reduction in cross sectional area. A top view of the necked specimen is illustrated in Fig. 6b and the data points in Fig. 6a can be projected onto it. Figure 6a clearly indicates that as the transducer interrogated the region of highest strain (minimum cross sectional area), the acoustic energy decreased. This confirms the results from the first data acquisition technique.

After the ultrasonic data were acquired, the specimens were sectioned and metallographically examined. The microstructure of the as-received alloy is shown in Fig. 7. The dark particles are Mg_2Si precipitates, while the lighter, more irregular particles are complex α-FeAlSi inclusions. These particles act as the sites for deformation induced void nucleation. The microstructure of a deformed specimen

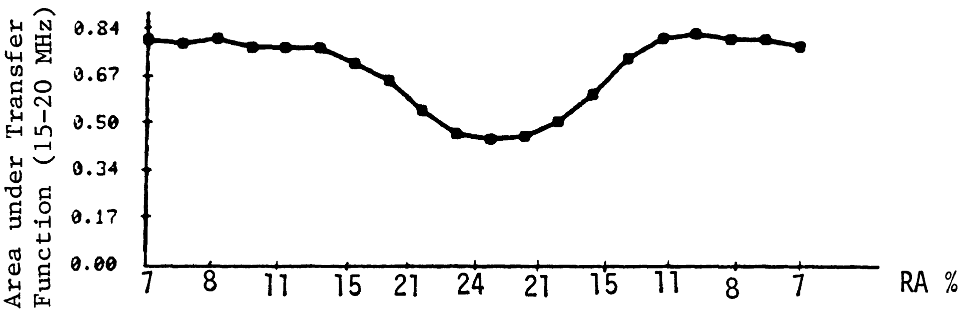

(a) Area under transfer function (15-20 MHz) versus reduction in cross sectional area (RA %).

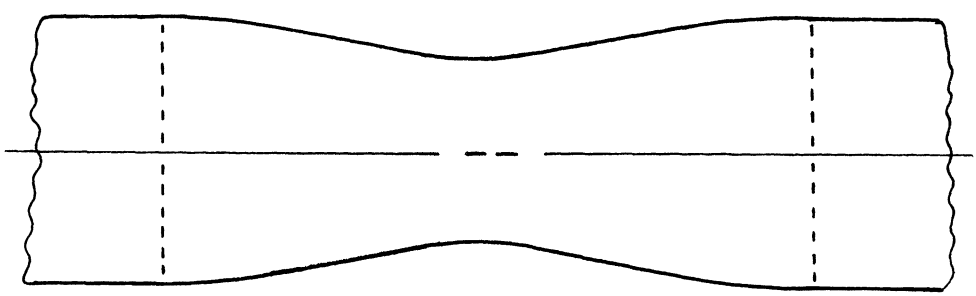

(b) Top view of neck region of tensile bar (area scanned is between dotted lines).

Figure 6. Ultrasonic signal amplitude vs. true strain in an aluminum (6061-T6) tensile bar.

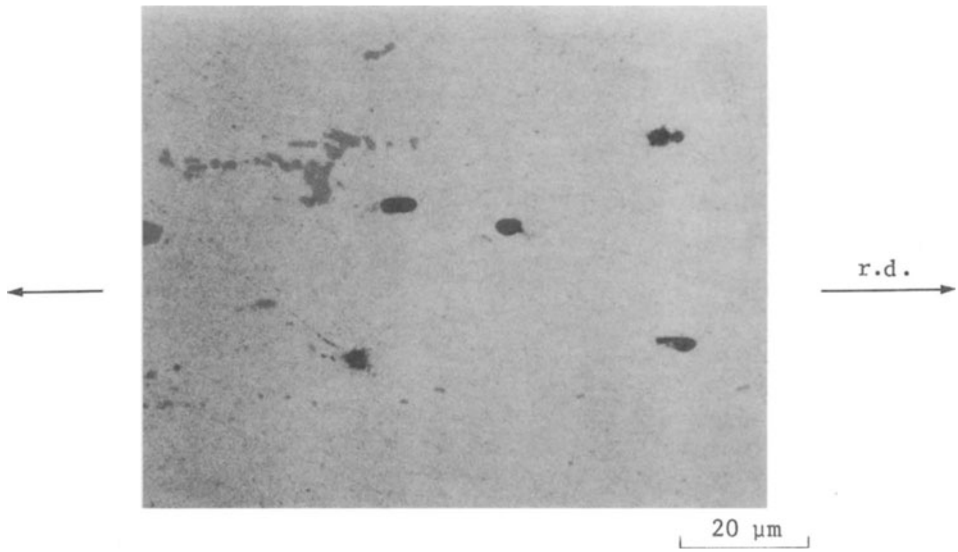

Figure 7. Microstructure of the as-received aluminum alloy (6061-T6). Dark spots are inhomogeneities. (R.D. = rolling direction).

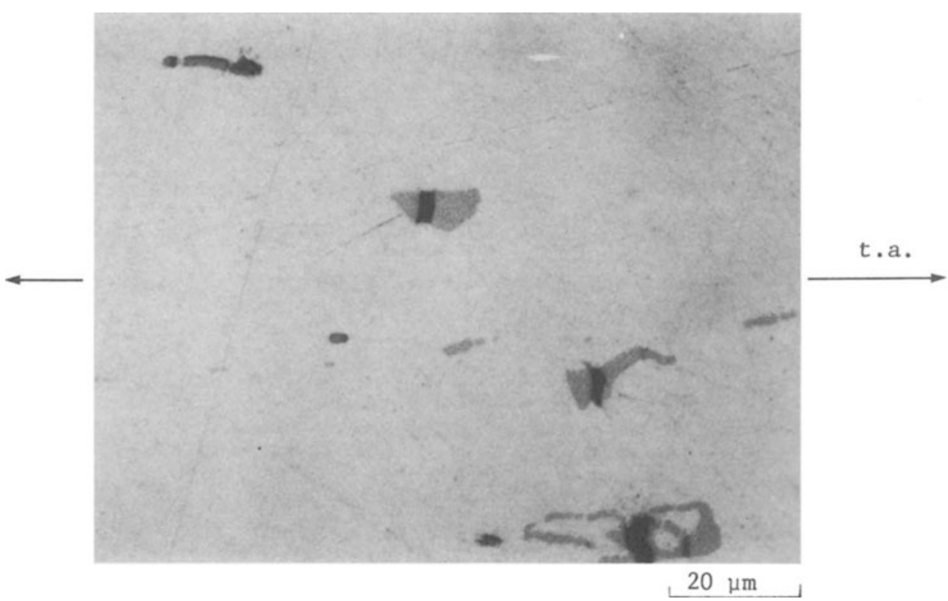

Figure 8. Microstructure of aluminum alloy after undergoing 16% strain. Black areas are where the particles have broken. (T.A. = Tensile Axis.)

is shown in Fig. 8, revealing the formation of voids which form principally as the result of particle fracture.

As stated earlier, these voids were scattering sites for the acoustic beam and their formation caused a decrease in the signal strength returning to the transducer. Preliminary metallography indicated that these voids appeared after approximately 5-8% strain. They were present in large quantities at strains approaching 15-20%. Thus the attenuation of the ultrasonic signal appeared to correlate with the onset of void formation. Additionally, the reflected acoustic energy returning to the transducer from the back wall of the specimen seemed to decrease as the void volume fracture increased.

FUTURE DIRECTIONS

Several future efforts are appropriate to studying the ultrasonic detection of deformation induced void nucleation. First a more exact quantification of ultrasonic attenuation measurements with void content and strain needs to be formulated. This entails accurate determination of void content and relating the content with an ultrasonic attenuation measurement. Secondly, the sensitivity and reliability of the ultrasonic measurement can be improved through a better understanding of the feature interactions. For example, one high frequency feature may be sensitive to the onset of void formation, but a lower frequency feature may dominate after substantial void growth. Thus a complex interaction of features may require a pattern recognition approach to gain the full benefit of this ultrasonic procedure. And lastly, other alloys and metals should be studied to determine the applicability of this technique to other materials.

REFERENCES

1. B.A. Wilcox and A.H. Clauer, "Creep of thoriated nickel above and below .5 T_m," Trans. of the AIME, Vol. 236, 570, 1966.
2. B.F. Dyson, M.S. Loveday and M.J. Rodgers, "Grain boundary cavitation under various states of applied stress," Proc. of the Royal Soc., Vol. 349A, 245, 1976.
3. J. Intrater and E.S. Machlin, "Grain boundary sliding and intercrystalline cracking," Acta Metallurgica, Vol. 7, 140, 1959.
4. K.E. Puttick, "Ductile fracture in metals," Philosophical Magazine, Vol. 4, 964, 1959.
5. D. Broek, "The role of inclusions in ductile fracture and fracture toughness," Engr. Frac. Mech., Vol. 5, 55, 1973.
6. T.C. Lindley, T. Oates and C.E. Richards, "A critical appraisal of carbide cracking mechanisms in ferride/carbine aggregates," Acta Metallurgica, Vol. 8, 1127, 1970.
7. J.D. Atkins, Ph.D. Thesis, University of Cambridge, 1973.

8. S.H. Goods and L.M. Brown, "Overview #1. The nucleation of cavities by plastic deformation," Acta Metallurgica, Vol. 27, 1, 1979.
9. A.S. Argon, J. Im and R. Safoglo, "Cavity formation from inclusions in ductile fracture," Metallurgical Trans., Vol. 6A, 814, 1975.
10. A. Vary, "The feasibility of ranking material fracture toughness by ultrasonic attenuation measurements," J. of Testing and Eval., Vol. 4, No. 4, 251-256, July 1976.
11. M. Rosen, et al., "An investigation of the precipitation-hardening process in aluminum alloy 2219 by means of sound wave velocity and ultrasonic attenuation," Mat. Sci. and Engr., 53, 1963-177, 1982.
12. S. Serabian, "Frequency and grain size dependency of ultrasonic attenuation in polycrystalline material," Brit. J. of Nondes. Test., Vol. 22, No. 2, 69-77, 1980.
13. A. Vary, "Computer signal processing for ultrasonic attenuation and velocity measurements for material property characterizations," Proc. of the 12th Symp. on Nondes. Eval., ASNT, Columbus, OH, 33-46, 1979.
14. E.P. Papadakis, "Ultrasonic attenuation caused by scattering in polycrystalline metals," J. of the Acous. Soc. of America, 37, 711-717, April 1965.
15. J. Shyne, et al., "Characterization of microstructure by acoustic NDE," Research on Nondestructive Testing, Final Report, AFOSR Grant No. AFOSR-78-3726, October 1979, G.L. Report No. 3049.
16. R. Bracewell, The Fourier Transform and Its Applications," McGraw-Hill, New York, 1973.
17. G.H. Thomas and J. Rose, "An ultrasonic evaluation and quality control tool for adhesive bonds," J. of Adhesion, Vol. 10, 1980.